ChemPhotoChem

Research Articles
doi.org/10.1002/cptc.202300070

Chemistry Europe
European Chemical Societies Publishing

www.chemphotochem.org

Water-Soluble Cationic Perylene Diimide Dyes as Stable Photocatalysts for H_2O_2 Evolution

Maciej Gryszel,[a, b] Tim Schlossarek,[c] Frank Würthner,*[c] Mirco Natali,[d] and Eric Daniel Głowacki*[a, e]

Photocatalytic generation of hydrogen peroxide, H_2O_2, has gained increasing attention in recent years, with applications ranging from solar energy conversion to biophysical research. While semiconducting solid-state materials are normally regarded as the workhorse for photogeneration of H_2O_2, an intriguing alternative for on-demand H_2O_2 is the use of photocatalytic organic dyes. Herein we report the use of water-soluble dyes based on perylene diimide molecules which behave as true molecular catalysts for the light-induced conversion of dissolved oxygen to hydrogen peroxide. In particular, we address how to obtain visible-light photocatalysts which are stable with respect to aggregation and photochemical degradation. We report on the factors affecting efficiency and stability, including variable electron donors, oxygen partial pressure, pH, and molecular catalyst structure. The result is a perylene diimide derivative with unprecedented peroxide evolution performance using a broad range of organic donor molecules and operating in a wide pH range.

Introduction

Photocatalytic synthesis of H_2O_2 is a concept widely investigated by researchers in recent years.[1,2] Such a light-driven process is interesting for solar energy conversion, where light is converted to the high-energy molecule H_2O_2, which can be used to drive single-compartment fuel cells.[3,4] The other application is biotechnology and biomedicine, where light is a versatile tool to generate on-demand peroxide for modulating cell signalling.[5–7] Although many different materials have been reported as photocatalysts for photoreduction of dissolved oxygen to peroxide (e.g. C_3N_4, TiO_2 or semiconductive organic pigments),[8–12] there are only a handful of examples of water-soluble dyes used for this purpose, despite their possible advantages.[13] Compared to solid materials, used in a form of planar layers or dispersed in a solvent, where only the surface is catalytically active, molecular photocatalysts demonstrate relatively higher number of catalytically active sites and have no requirement of intermolecular charge carrier transport. Some of us introduced this concept of peroxide photogenerating dyes in 2019.[13] This concept of organic dye solutions used for photocatalytic peroxide generation is relatively novel, save for this 2019 work, to the best of our knowledge. There, three dyes were presented (representing different chemical classes), which if irradiated in a water mixture with sacrificial electron donor, reduce O_2 to H_2O_2. We proved that the process (schematized in Figure 1a) involves dyes as photocatalysts in their molecular (i.e. not aggregated) form and peroxide is generated via the metastable superoxide intermediate (product of $1e^-$ Oxygen reduction reaction (ORR)). In this work, based on our previous findings and knowledge on redox properties of core-substituted PDI dyes,[14,15] we are aiming for materials of higher catalytic performance and higher stability.

Although in our initial study, the best dye (in terms of H_2O_2 concentration and stability) was a naphthalene diimide derivative, due to its high bandgap we decided to focus on the perylene diimide core with wider visible light absorption. The main limitation of the dye from this class which we investigated in 2019, **PDI-S** (shown in Figure 1b), was its tendency to aggregation, a common feature for this class of pigment-forming dyes.[16] Although it forms stable solutions in pure water, it precipitates from mixtures with other compounds (especially ionic) and loses its photoactivity. This makes it difficult to utilize sacrificial electron donors in the process. Therefore, we were motivated to consider alternative solubiliz-

[a] Dr. M. Gryszel, Dr. E. D. Głowacki
Warsaw University of Technology
Faculty of Chemistry
Noakowskiego 3, 00-664 Warsaw (Poland)
E-mail: eric.glowacki@pw.edu.pl
[b] Dr. M. Gryszel
Laboratory of Organic Electronics
Department of Science and Technology
Linköping University
Norrköping, Bredgatan 33, 60174 Norrköping (Sweden)
[c] T. Schlossarek, Prof. F. Würthner
Institut für Organische Chemie and Center for Nanosystems Chemistry
Universität Würzburg
Am Hubland, 97074 Würzburg (Germany)
E-mail: wuerthner@uni-wuerzburg.de
[d] Prof. M. Natali
Department of Chemical, Pharmaceutical and Agricultural Sciences
University of Ferrara
Via L. Borsari 46, 44121 Ferrara (Italy)
[e] Dr. E. D. Głowacki
Bioelectronics Materials and Devices Laboratory
Central European Institute of Technology
Brno University of Technology
Purkyňova 123, Brno 61200 (Czech Republic)
E-mail: eric.daniel.glowacki@ceitec.vutbr.cz

Supporting information for this article is available on the WWW under https://doi.org/10.1002/cptc.202300070

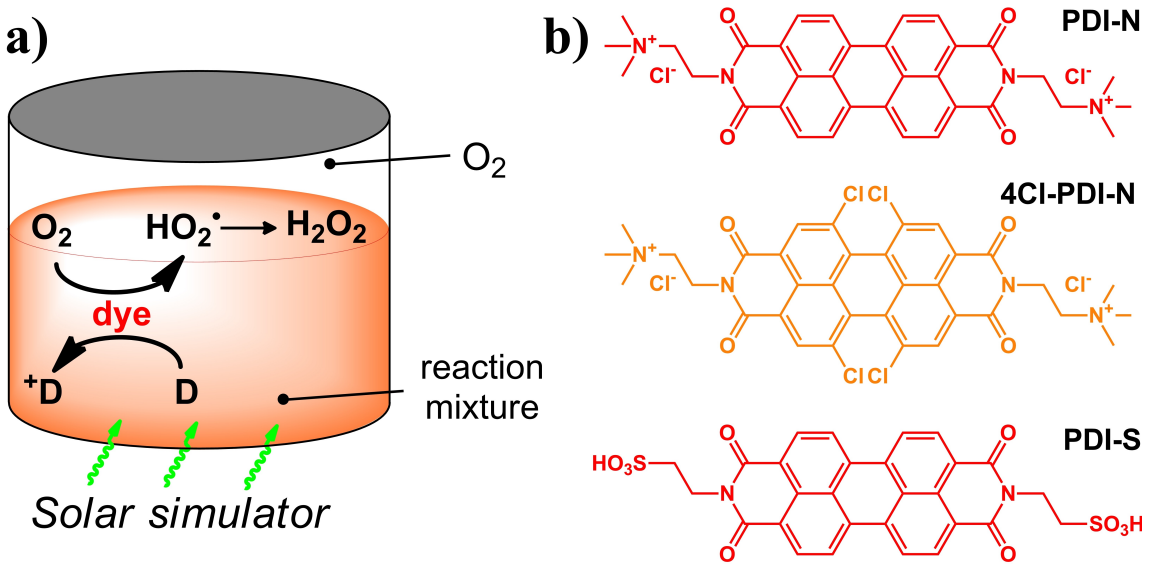

Figure 1. a) Schematic of H_2O_2 photogeneration with an aqueous dye molecular catalyst. An oxygenated water solution of the dye, containing sacrificial electron donor (D), is irradiated with a solar simulator (105 mW/cm^2). H_2O_2 is generated as the result of disproportionation of $HO_2^{\bullet}$, the unstable intermediate oxygen reduction product. b) Chemical structure of **PDI-N** and **4Cl-PDI-N**, the dyes investigated in this work. As a reference, we show the structure of **PDI-S**, the compound used in our previous study. Color of the structures corresponds to the approximate color of their aqueous solutions.

ing units to yield more aggregation-resistant PDI-based photocatalysts. Herein, the original solubilizing unit, R-SO_3^- was replaced with quaternary ammonium, R-N$(CH_3)_3^+$, charge-balanced by Cl^- anion. This should not only limit precipitation of the dye, but also facilitate its interaction with negatively charged sacrificial electron donors. Attempting to limit light-induced self-oxidation of the photocatalysts, we also modified the structure of the perylene core by chlorine substitution in the 1,6,7,12-positions. Incorporation of these bulky substituents in the bay area induces a rotational displacement between the two naphthalene units of the PDI core.[17] As a result, the tendency for self-aggregation is significantly reduced for these chromophores[18] compared to unsubstituted parent PDI that is also subject in this study. Additionally, the electron-withdrawing nature of the chlorine substituents should lower the HOMO energy, thereby improving the photostability of the catalyst.[12] Chemical structures of the two new dyes investigated in this paper, **PDI-N** and **4Cl-PDI-N**, are presented in Figure 1b. Although synthesis of such dyes is already reported in the literature,[19] to the best of our knowledge, they were never tested as photocatalysts. We have found that these molecules exceed the catalytic performance and stability of the report on dye-based photocatalytic peroxide evolution and demonstrate competitive values of peroxide production which are well in the range desired for many biochemical and biological experiments.

Results and Discussion

The synthesis of the dyes was performed in three steps, starting from perylene dianhydride or its tetrachloro-substituted counterpart. The details on the synthesis and materials characterization can be found in the supporting information part I, Figures S1–S12. As expected, **PDI-N** and **4Cl-PDI-N** demonstrated high solubility in water with the formation of true solutions, not dispersions of nanoparticles, as determined with dynamic light scattering (DLS). Using concentration- and temperature-dependent UV-Vis spectroscopy, we compared the aggregation properties of both dyes. The results, presented in Figure 2 and Figure S13–S14, indicate that the bay substitution hampers the aggregation whilst **PDI-N** shows a concentration- and temperature-dependent self-assembly process into H-type aggregates (for further information, see supporting information) as evidenced by the decrease of the 0,0 transition at 532 nm and a concomitant increase of the higher energy vibronic transitions.[20] Similar spectral changes have been observed for other PDI aggregates both in organic solvents and in water and were attributed to the formation of rotationally twisted π-stacks.[21] The absence of such spectral changes for **4Cl-PDI-N** suggests that these dyes prevail as monomers and therefore should outperform its unsubstituted counterpart in H_2O_2 photoevolution.

To test if **PDI-N** and **4Cl-PDI-N** do not precipitate from solutions containing sacrificial electron donors, their mixtures (at different pH) were left in the dark for the expected duration of the photoexperiments. Monitoring the progress of the aggregation with UV-Vis spectroscopy and DLS measurements, we observed different results depending on the pH of the solution. All pH 2 and pH 7 samples showed very stable optical spectra (shown in Figure S16–S19) and very weak light scattering signal. As shown in the example presented in Figure S20, this proves considerably improved stability of the solutions compared with **PDI-S**. At pH 12, the description of aggregation properties is more complex, especially in the case of**4Cl-PDI-N**. Shortly after adjusting the pH of its pure solution, the color,

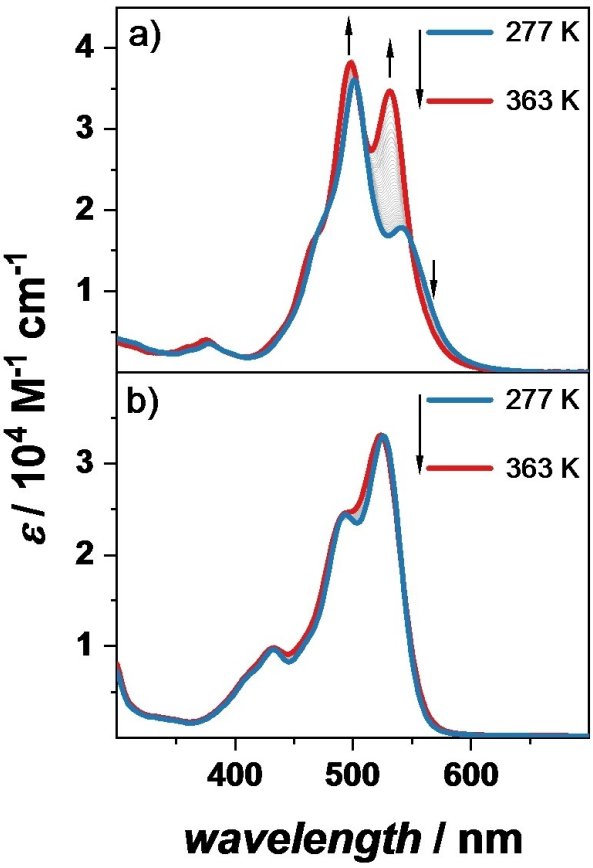

Figure 2. Temperature-dependent UV = Vis absorption spectroscopy of aqueous solutions of **PDI-N** (a) and **4Cl-PDI-N** (b) in a temperature range from 277 K to 363 K (2nd heating). Arrows indicate spectral changes observed during the heating process.

originally orange, turns yellow. This results in a significantly altered UV-Vis spectrum, shown in Figure S21. The process is reversible upon neutralization to pH 7 and, as described in more detail in the supporting note 1, is caused by formation of aggregates. Although the aggregation might have an impact on efficiency of H_2O_2 evolution at pH 12, it is worth noting that this is still considerable improvement compared with **PDI-S**, which in basic solutions tends to create colloidally unstable suspensions of >10 μm diameter particles.

Testing the performance of the dyes as photocatalysts for H_2O_2 evolution, we applied the same methodology like in our previous works, with the setup schematized in Figure 1a. Aliquots of the irradiated solutions were taken over the course of the experiments to measure peroxide concentration with HRP/TMP assay. Experimental details can be found in the supporting information, part II. Considering improved stability against precipitation of **PDI-N** and **4Cl-PDI-N**, we hypothesized that they should demonstrate photocatalytic activity with a higher number of sacrificial electron donors than **PDI-S**. Indeed, it turned out that the new dyes photogenerate H_2O_2 with wide variety of different organic donor compounds, in broad range of pH. We observed photocatalyzed H_2O_2 evolution with alcohols (methanol, ethanol, isopropanol, benzyl alcohol), lactic acid, propionic aldehyde, and various amines. Therefore, apart from hydrogen peroxide synthesis, the dyes can be possibly utilized for photocatalytic removal of organic pollutants. Although oxalate is the best donor in terms of the H_2O_2 production rate, it works optimally only at relatively low concentration (see supporting note 2 for additional information) what impedes accumulation of peroxide due to depletion of the donor. To avoid this limitation, aiming for high H_2O_2 concentrations, we performed experiments with ternary amines (such as triethylamine and triethanolamine) seeing that they retain high activity in a wide range of concentrations. The best of them overall was HEPES, which gave almost 22 mM in 20 h in the photoreaction catalysed by **4Cl-PDI-N**. HEPES is a non-toxic buffering agent widely used in cell culture, and as such represents a particularly useful donor for biological research applications. Although it is reported to produce H_2O_2 with ambient light without presence of external photocatalysts,[22] we detected only trace amounts of peroxide in pure HEPES solution irradiated with our LED solar simulator (i.e. not emitting UV), proving high photocatalytic activity of the dyes. Selected results, as concentrations of H_2O_2 over the irradiation time, are presented in Figure 3. Compared with the previously investigated **PDI-S**, both **PDI-N** and **4Cl-PDI-N** are significantly more active, resulting in 4–60 times higher H_2O_2 concentration (depending on the pH and donor) for the same experiment duration.

In many cases, the shape of the peroxide evolution curve indicates that over the course of the experiment, H_2O_2 synthesis slows down. It is mostly the result of progressing degradation of the dye and consumption of the donor, but in H_2O_2-rich mixtures there is also an issue of competitive reaction of H_2O_2 to H_2O reduction. As proved in our previous works, this is a common problem with concentrated solutions of H_2O_2, caused by relatively low oxygen solubility in water (ap. 1.2 mM in pure H_2O under 1 bar O_2 pressure[23]), resulting in decreased efficiency of peroxide production. To avoid this limitation and achieve even higher H_2O_2 concentrations, we performed photo-experiments under elevated pressure of oxygen. According to Henry's law, solubility of a gas in liquid is directly proportional to its partial pressure above the liquid. We employed a commercially available Büchi Tinyclave Type 1 glass reactor, allowing to run the process with pressure up to 11 bar. Pictures of the setup are presented in Figure S23. Although the concept of utilizing pressurized reactor was already tested for electrochemical O_2 to H_2O_2 reduction,[24,25] we have not found any reports on photocatalytic H_2O_2 evolution at elevated O_2 pressure. We believe we present the first example in this work. Based on the data presented in Figure 3, for the high-pressure experiments were selected **4Cl-PDI-N** and HEPES at pH 7. To provide a sufficient amount of sacrificial electron donor, its concentration was increased; we also tested the H_2O_2 photo-evolution with higher dye concentration (75 μM). Measurements were run with stronger light source (300 mW/cm^2) to increase throughput and shorten the experiment time. The results presented in Figure 4 prove that while maintaining the same conditions, reaction rate and final concentration of H_2O_2 can be significantly increased just by making the solution more oxygen-rich. The concentration of peroxide close to 83 mM

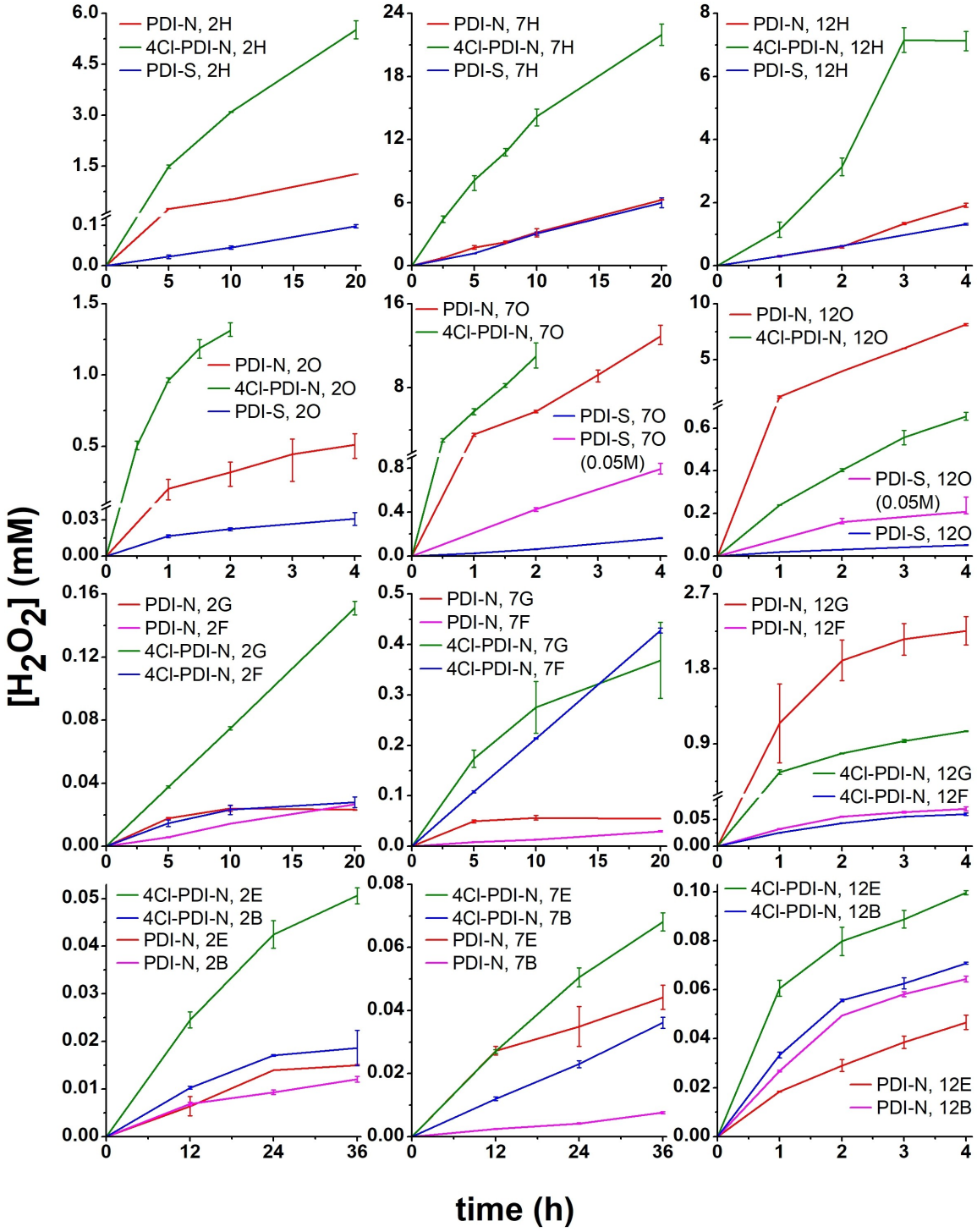

Figure 3. H_2O_2 concentrations over time of dye-photocatalysed O_2 reduction. The experiment duration depends on photostability of dyes (always 50 μM) at given conditions. Traces in plot legends are labelled such that the number is pH of the solution, while the letter stands for sacrificial electron donors used at following concentrations: B – blank (without any donor), E – 1 M ethanol, F – 0.1 M formate, G – 0.4 M glucose, H – 0.03 M HEPES, O – 0.02 M oxalate. For reference, available **PDI-S** data (depending on its activity at given conditions) is added to some plots. For oxalate, we also present **PDI-S** data for 0.05 M (optimal for this dye).

were measured for the solution containing 75 μM **4Cl-PDI-N** and 100 mM HEPES concentration is, to our best knowledge, the highest ever reported for photocatalytic O_2 reduction. The experiment proves that oxygen concentration is the limiting factor rather than dye stability. It is worth noting that having appropriate equipment, running the reaction at elevated pressure presents no challenges and it is common practice in many areas of chemical and biotechnological industries.

As shown in Figure S16–19, in contrast to samples kept in dark, over the course of the photoexperiments we registered

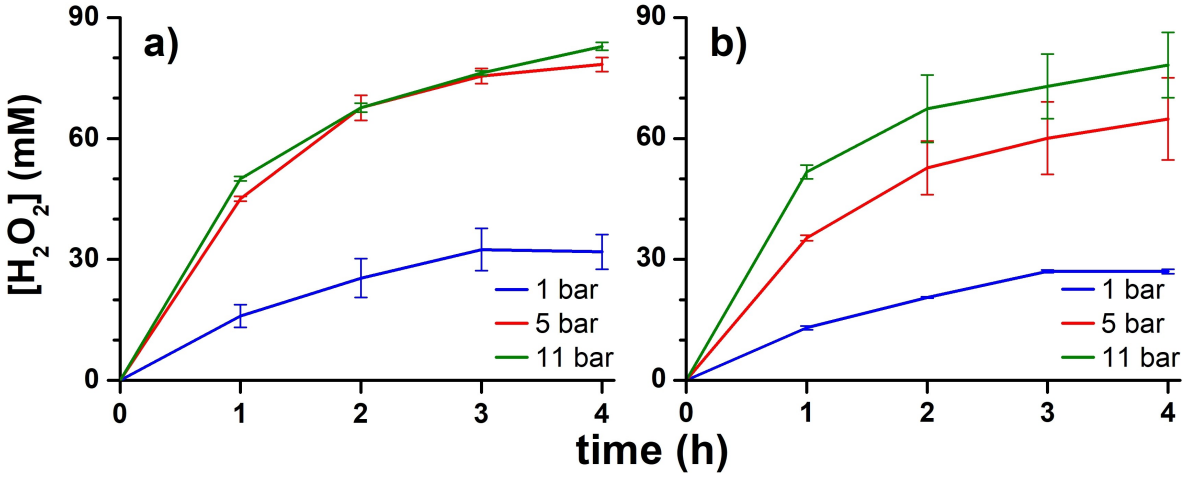

Figure 4. H_2O_2 concentrations in photoevolution (pH 7, 300 mW/cm^2 irradiance) under elevated pressure of gaseous O_2. a) [**4Cl-PDI-N**] = 75 μM, [HEPES] = 0.1 M. b) [**4Cl-PDI-N**] = 50 μM, [HEPES] = 0.2 M. With abundance of reagents and light, the main limitation is stability of the dye. After 4 h of the experiment, solutions are almost completely bleached.

significant changes in UV-Vis spectra. This indicates occurrence of chemical degradation of the photocatalysts. Therefore, like in our previous works on photocatalytic H_2O_2 evolution, we calculated catalytic turnover numbers (TON), defined as the ratio of molar amounts of generated H_2O_2 and degraded dye. Considering much higher precipitation resistance of **4Cl-PDI-N** and **PDI-N**, in many cases degradation of the dye could be simply evaluated based on the absorbance measurements performed directly on the irradiated solutions. Nevertheless, we decided to stick to the previously introduced method with UV-Vis measurements performed after changing the solvent from water to concentrated H_2SO_4. This allows to apply the same approach also to pH 12 samples, which have different and unstable UV-Vis spectra, as described in the supporting note 1. The values of TON are presented in Figure 5.

Highest TONs are achieved with HEPES and oxalate, what serves as another proof (along with high H_2O_2 concentration) of their usefulness in the photocatalytic H_2O_2 generation. On the other hand, low turnover numbers (0.8 to 2.6) for samples without sacrificial electron donors indicate that the dyes are not able to utilize water as a source of electrons for the ORR and undergo autooxidation. The protective effect of the sacrificial electron donor presence can also be seen in Figure S24, showing the results of H_2O_2 photoevolution (**4Cl-PDI-N**, pH 7) with increasing concentration of HEPES. We see not only improved efficiency of peroxide production, but also higher TONs.

In our previous studies with organic semiconductors and water-soluble dyes, we found that the lower the HOMO level, the higher its stability measured as TON. To see if the same rule applies to the dyes investigated in this work, we calculated their HOMO levels using cyclic voltammetry and UV-Vis spectroscopy. Details are presented in the supporting information part I (Table S1 and Figure S15). As expected, **4Cl-PDI-N** is

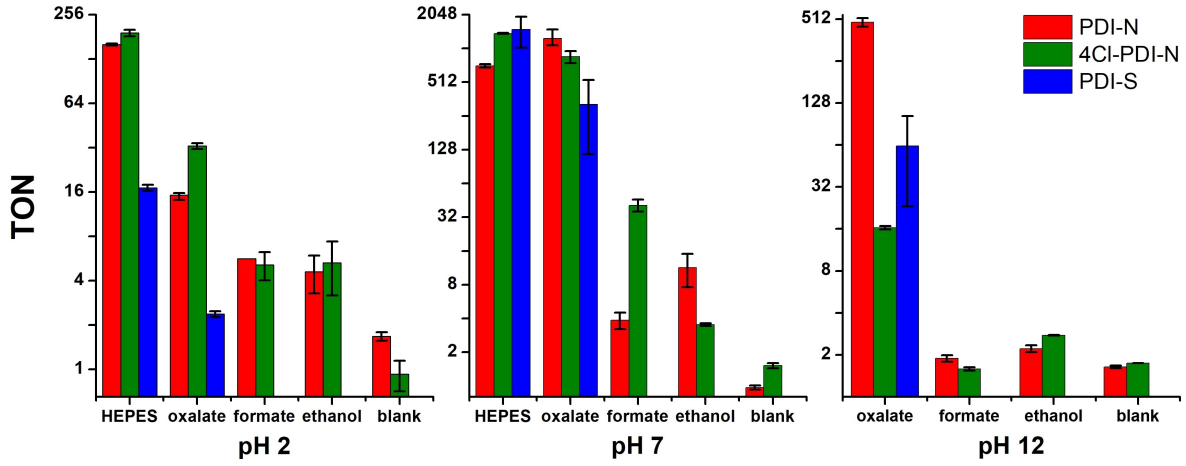

Figure 5. Turnover numbers (TONs) in photocatalytic H_2O_2 evolution at different conditions. Calculations were based on H_2O_2 concentration and dye degradation, evaluated with UV-Vis spectroscopy of the samples dissolved in concentrated H_2SO_4. Application of this method was impossible for samples containing glucose (all pH values) and HEPES (at pH 12) due to their spectral mismatch with the references. Available **PDI-S** data is provided for comparison, depending on activity of this dye at given conditions.

a compound of slightly lower HOMO level than **PDI-N** (−6.92 vs. −6.70 eV). However, as it can be seen in Figure 5, there is no clear correlation between HOMO levels and stability measured as TON. This shows that in some cases, especially if the difference in HOMO levels is small, there are other factors impacting stability. Nevertheless, overall turnover numbers of both **PDI-N** and **4Cl-PDI-N** are on average higher than measured for **PDI-S**, indicating higher photostability of the new structures.

Although H_2O_2 is a product of $2e^-$ reduction of oxygen, in our previous study on photocatalytic dyes, we proved that peroxide is synthesized via superoxide intermediate, a product of $1e^-$ ORR. This conclusion was based on measurements of the reaction kinetics using the method of initial rates and hypothesized mechanisms involving the reaction of the excited dye with oxygen, presented in the supporting note 3 as *pathway 1*. This assumption seemed reasonable considering that for the samples without sacrificial electron donor we observed H_2O_2 evolution, albeit with low efficiency and high dye degradation. However, in the presence of sacrificial donors, literature suggests an alternative pathway,[26,27] with the photo-excited PDI molecule first reacting with the electron donor and the photogenerated PDI radical anion afterwards reducing oxygen (*pathway 2* in the supporting note 3). To determine which mechanism is occurring for H_2O_2 photoevolution with **PDI-N** and **4Cl-PDI-N**, we performed emission quenching experiments (see supporting note 3). With increasing HEPES concentration, a concomitant proportional decrease in both emission intensity and excited state lifetime was observed. This is consistent with a dynamic quenching process of the excited state by electron transfer from the HEPES donor to the singlet excited state of the PDI chromophore. For **4Cl-PDI-N**, Stern-Volmer analysis yields bimolecular rate constants in the diffusion-controlled regime. On the other hand, the similar lifetimes measured in both oxygenated and deoxygenated conditions confirm that excited state quenching by oxygen is, if any, of low efficiency. These findings strongly imply occurrence of *pathway 2*, with oxygen being reduced by the anionic form of the dye. This hypothesis is further corroborated by UV-Vis spectroscopy of the deoxygenated mixtures of **PDI-N** and **4Cl-PDI-N** subjected to irradiation in the presence of donor. Results, shown in Figure S29, prove the formation of PDI radical anions that are very sensitive to oxygen. Importantly, the dependence of the excited state quenching yield and concurrent PDI radical anion photogeneration on the concentration of the donor, as expected for *Pathway 2*, also explains why the increasing concentration of HEPES not only leads to higher turnover numbers, but also to faster H_2O_2 evolution (as shown in Figure S24).

Occurrence of the dye-catalysed ORR via *pathway 2* does not exclude the possibility of H_2O_2 generation by other processes. Apart from oxygen reduction by the oxidation products of sacrificial electron donors (e.g. $CO_2^{\bullet-}$ in the case of oxalate[28]), we also considered the possibility of H_2O_2 synthesis via type II photoprocess involving singlet oxygen. If that is the case, at first the dyes photogenerate singlet oxygen, which oxidises a donor and turns to H_2O_2 in a second step without involvement of light.[29] To verify if such mechanism is possible with **PDI-N** and **4Cl-PDI-N**, we employed commercially available singlet oxygen sensor green, a compound which selectively reacts with $^1O_2$ giving a fluorescent product. It shows no response to superoxide or H_2O_2.[30] Details can be found in supporting note 4. We verified the sensor activity by irradiation (520 nm LED) of its oxygenated mixture with rose Bengal, well-known singlet oxygen photosynthesizer. However, we detected no $^1O_2$ when **PDI-N** or **4Cl-PDI-N** were tested in the same way. We also performed selected H_2O_2 photoevolution experiments with dyes and sacrificial electron donors dissolved in 1:1 mixture of H_2O and D_2O (known of increasing lifetime of $^1O_2$), with no increase of peroxide production efficiency. These findings suggest that the investigated dyes are not able to photogenerate singlet oxygen, despite previous reports of this process for other perylene dyes.[31,32] However, in these studies, the $^1O_2$ assay involved DPBF sensor, which is not selective and reacts also with superoxide[33] and hydrogen peroxide.[34] Considering that these works were based on irradiation of alcohol containing solutions, it is possible that these dyes, similarly to **PDI-N** and **4Cl-PDI-N**, photogenerated $O_2^{\bullet-}$ and H_2O_2. This would trigger the reaction of DPBF which could be mistaken as a false positive for $^1O_2$ photosensitization.

Conclusions

In summary, we conclude that **PDI-N** and **4Cl-PDI-N**, perylene diimide derivatives with quaternary ammonium solubilizing units, demonstrate high resistance to precipitation and significantly improved performance and versatility in H_2O_2 evolution compared with previously investigated dyes. This is an important finding in the search for molecular peroxide producing photocatalysts showing high long-term stability. We did not find any evidence supporting the idea that the dyes act as photosensitisers for generation of singlet oxygen, which contradicts previous reports concerning other compounds of perylene diimide-based structure. We also proved that in highly concentrated solutions of H_2O_2, low solubility of O_2 in the reaction mixture is a major factor limiting efficiency of peroxide evolution, possible to overcome by increasing pressure of gaseous oxygen. To raise peroxide yields, catalyst loading would have to be improved via increased solubility without aggregation, perhaps aided by surfactants. The quantum efficiency of photon-to-peroxide conversion remains low, $<1\%$ quantum efficiency, even after correcting for absorption. While this molecular approach may not be the best route to photosynthesis of peroxide from dissolved oxygen, it could be very promising in biotechnological/biophysical applications. Consideration of the degradation products of specific donor molecules used to complete the redox cycle may be important for certain experiments. On-demand reactive-oxygen species generation is vital to many processes, and concentrations in the range of 1–1000 μM is desired for biophysical research.[7,35,36] This route using molecular organic dyes gives a "clean" source of peroxide, without singlet oxygen generation. From a thermodynamic point of view, these types of molecular dye catalysts

may also be considered for driving other useful photocatalytic transformations, such as hydrogen evolution, or reduction of CO_2.

Experimental section

General

All reagents and solvents were purchased from commercial sources and used without further purification. Dry solvents were obtained from the solvent purification system PS-M6-6/7 (*inert technologies*).

NMR spectroscopy

^{1}H NMR spectra were recorded on an Avance III HD 400 spectrometer (*Bruker Daltonics GmbH*) operating at a temperature of 295 K and a frequency of 400 MHz (^{1}H). Chemical shifts (δ) are stated in parts per million (ppm) using the residual solvent signal for calibration against TMS and coupling constants J are given in Hz. Multiplicities are described as singlet (s), doublet (d), triplet (t) or multiplet (m).

Mass spectrometry

High-resolution ESI-TOF measurements were performed on an ESI MicrOTOF focus mass spectrometer (*Bruker Daltonics GmbH*). MALDI-TOF measurements were carried out on an UltrafleXtreme spectrometer (*Bruker Daltonics GmbH*) using *trans*-2-[3-(4-tert-butylphenyl)-2-methyl-2-propenylidene]-malononitrile (DCTB) as matrix.

Electrochemistry

Cyclic voltammetry (CV) and differential pulse voltammetry (DPV) measurements were performed on a BAS Cell Stand C3 (*BAS Epsilon*) using a three-electrode setup with a platinum working and auxiliary electrode and a silver reference electrode. Experiments were carried out in acetonitrile with tetrabutylammonium hexafluorophosphate (0.1 M) as supporting electrolyte and the ferrocenium/ferrocene (Fc^+/Fc) redox couple as internal standard.[37]

UV-Vis absorption spectroscopy – characterization of the dyes

UV-Vis spectra were recorded on a V-770 UV/Vis/NIR spectrophotometer (*Jasco Inc*) using Suprasil quartz cells with varying pathlengths that were silanized before use due to adsorption of the dyes on glass surface. Solutions were prepared using spectroscopy grade solvents (acetonitrile) or doubly distilled water that was obtained by passing distilled water through a Millipore filter system. Absorptivities are converted into extinction coefficients using the Beer-Lambert law.

Atomic force microscopy

AFM measurements were performed under ambient conditions using a Multimode 8 SPM system (*Bruker Daltonics GmbH*) operating in tapping mode under air. Silicon cantilevers (*OMCL-AC240TS, Olympus*) with a resonance frequency of ~70 kHz and a spring constant of ~1.7 Nm^{-1} were used. For preparation of AFM samples, the solution of **PDI-N** and **4Cl-PDI-N** in water (pH 7 or pH 12) with a concentration of 50 μM was spin-coated onto mica substrates with 7000 rpm.

Steady-state fluorescence spectroscopy

Fluorescence spectroscopy was carried out on an FLS980 fluorescence spectrometer (*Edinburgh Instruments*) using Suprasil quartz cells with a path length of 1 cm. Measurements were carried out using the magic angle setup in doubly distilled water that was obtained by passing distilled water through a Millipore filter system. Measurements of deoxygenated solutions were carried out after degassing the solutions with argon in a cuvette with Schlenk cap. Lifetime measurements were performed using time correlated single photon counting (TCSPC) using an EPL picosecond pulsed diode laser ($\lambda_{Fl} = 505.8$ nm) with a pulse width of 141.7 ps. Data was fitted according to the Tail-Fit routine supplied by the manufacturer.

Synthesis

The synthesis of **PDI-N** and **4Cl-PDI-N** (Scheme 1) was accomplished according to slightly modified published procedures in similar yields. The collected analytical data are in accordance with the published data.[19,38–40]

UV-Vis spectroscopy – experiments with sacrificial electron donors

In the case of dyes mixtures with sacrificial electron donors (both irradiated and not irradiated) and samples dissolved in conc. H_2SO_4 (for determination of TON, see separate section below), UV-Vis spectra were recorded with a Synergy H1 Microplate reader (BioTek® Instruments, Inc.) using 96-Well Polystyrene flat bottom plates. Volume of the sample was always 300 μL.

Dynamic light scattering measurements:

Using Malvern Zetasizer Nano ZS90 Dynamic Light Scattering instrument with disposable PS micro cuvettes, we attempted to measure size of the dyes aggregates/particles. However, in the case of almost all mixtures of the dyes with sacrificial electron donors, we failed to record any data due to insufficient signal strength - count rate (number of scattered photons) was out of range. This indicates that either the samples are free of aggregates or that their "scattering effect" (impacted by both aggregate size and concentration) is too weak for the instrument to register. The only exception were pH 12 HEPES solutions (both irradiated and not irradiated **PDI-N** and **4Cl-PDI-N**), where the count rate was sufficient, but the resulting data was of poor quality, making the particle size determination impossible. It is worth noting that for **PDI-S**, DLS signals were obtained with all sacrificial electron donors and at all pH values, showing that the new perylene structures are less prone to form precipitates, thus, are better suited for H_2O_2 photocatalysis.

H_2O_2 photoevolution – experiments at atmospheric pressure

In photocatalytic experiments, we used stock solutions of **PDI-N** and **4Cl-PDI-N** (100 μM; kept in polypropylene bottles at room temperature in dark) and stock solutions of sacrificial electron donors (double the concentration as listed in the main article). The mixtures were always prepared just before the experiment by adding 400 μL of a dye and 400 μL of a sacrificial electron donor to a 4 mL silanized (*n*-octyltriethoxysilane) borosilicate white glass

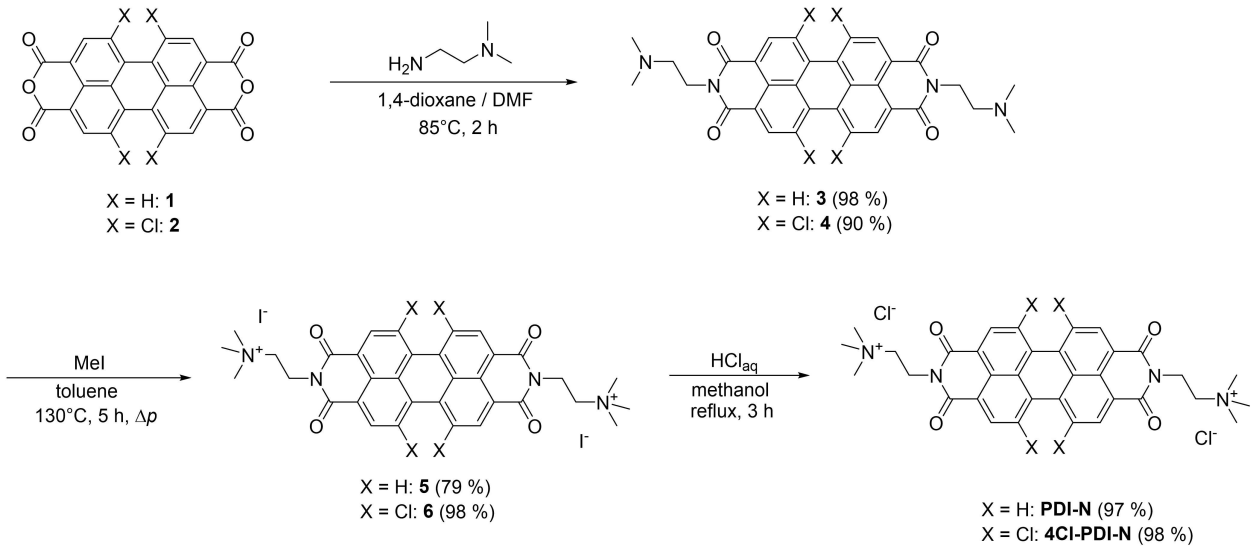

Scheme 1. Synthetic scheme to obtain dichloride salts of the trimethylammonium substituted derivatives **PDI-N** and **4Cl-PDI-N**, respectively.

vials with a PTFE/rubber septum stopper. The samples were illuminated with a white LED lamp (electrical input 30 W, round shape white LED array (27 mm Ø) with matte glass placed 50 mm above, giving a platform with uniform light of intensity of 1.05 sun (105 mW cm^{-2}) at the point where vials are placed). The system is equipped with a fan (120 mm Ø) to maintain room temperature. Before starting the irradiation and each time the vials were opened to take an aliquot of the solution (to measure H_2O_2 concentration over the course of the experiment), they were flushed with stream of water-saturated oxygen (60 s, flow 100 ml min^{-1}) using steel needles as inlet and outlet, pierced through the stopper of the vial. All experiments were performed 2–4 times for given type of the sample. The resulting H_2O_2 concentrations (presented in Figure 3 and 4) are averaged, the error bars provided are delimited by max. and min. H_2O_2 concentration for given condition.

H_2O_2 photoevolution – high pressure experiments

Photocatalytic H_2O_2 synthesis at elevated pressure of oxygen were performed in a similar way like at atmospheric pressure, with stock solutions of **4Cl-PDI-N** (100 μM) and HEPES (0.4 M), mixed at 3 : 1 or 1 : 1 ratio. Before experiments, the glass part of Büchi Tinyclave Type 1 glass reactor (25 mL) was treated with oxygen plasma (200 W, 10 min) and silanized at 80 °C with vapor of *n*-octyltrieth-oxysilane. After loading the reactor with 800 μL of the reaction mixture, it was pumped with oxygen to 5 bar (supplied from gas cylinder via *Swagelok* connectors) and quickly evacuated (by opening the valve to the atmosphere) to around 1.1 bar. The procedure was repeated 6 times to provide high purity of O_2 in the reactor when it was finally pumped to the desired pressure (1, 5 or 11 bar). During the photoreaction, the oxygen supply was disconnected, but with high gas to liquid ratio, O_2 consumption was negligible (as indicated by lack of pressure change during the photoreaction). Pumping procedure was repeated every time the reactor was open to take an aliquot of the solution to measure H_2O_2 concentration. The light source (the same like used in the experiments at atmospheric pressure) was put closer to the irradiated solution (ap. 20 mm), resulting irradiance was approximately 300 mW cm^{-2} (as measured with photodiode placed inside empty reactor; the effect of partial shadowing of the light beam by the anti-burst cage is therefore accounted for). Despite presence of cooling fans (shown in Figure S23), partial condensation of evaporated water could be noticed in the lower part of the reactor. Therefore, before each H_2O_2 measurements, the reaction mixture was spread (with a pipette) on the glass 3–4 cm above the solution.

Determination of hydrogen peroxide concentration

The quantification of the produced hydrogen peroxide was done spectrophotometrically by following the oxidation of 3,3′,5,5′-Tetramethylbenzidine (TMB) in presence of horseradish peroxidase (HRP) and citric acid – phosphate buffer solutions. Values of absorbance were measured at 653 nm with Synergy H1 Microplate reader (BioTek® Instruments, Inc.) in 96-Well Polystyrene flat bottom plates. Depending on hydrogen peroxide concentration in the sample, aliquots of different volumes (1–50 μL) were taken and added to the corresponding volume of HRP/TMB/buffer solution, in every case giving finally 300 μL of the solution. In the case of H_2O_2 solutions of high concentration (> 8 mM), before the assay, aliquots were prediluted (2–15 times) with deionized water. The obtained absorbance values were recalculated to concentration based on calibration curve formulas ($R^2 > 0.998$ in every case).

Determination of dye contents for turnover number calculation

At the end of photoexperiments, defined volume of the samples (500–750 μL) was transferred to 10 mL round bottom flask, along with 200 μL of 0.1 M phosphate buffer and 2 μL of catalase from bovine liver solution (2000–5000 units mg^{-1} protein; 1 mg ml^{-1} in 0.05 M PBS buffer) to decompose hydrogen peroxide. After > 15 min, rotary evaporator was used to remove water from the mixture to give solid residue which was sonicated for 5 min with 95 % H_2SO_4 (of the same volume like the starting **PDI-N** and **4Cl-PDI-N** sample and double the volume of **PDI-S** sample). Resulting violet solutions were subjected to UV-Vis measurements. When the obtained spectra were in agreement with the spectra of not-irradiated solutions, absorbance values at a maximum of the strongest peak (594 nm for **PDI-N**, 560 nm for **4Cl-PDI-N** and 596 nm for **PDI-S**) were recalculated to concentrations based on calibration curve formulas ($R^2 > 0.999$ in all cases). Finally, dye degradation was calculated as a difference between starting 50 μM

concentration and its concentration in a sample after H_2O_2 photoevolution. For each sample, the final results is average of 2–4 experiments, error bars provided in Figure 5 are delimited by max. and min. TON. The presented method is fast and convenient, but based on the assumption that degradation products of dyes do not absorb light at the abovementioned wavelengths. It is possible that with different method of dye quantification (e.g. based on HPLC), the obtained results would vary from the results presented in this paper. Aggregation effects were considered according to previously published methods.[41]

Acknowledgements

The authors are grateful for support from the National Science Centre, Poland, within grant 2019/33/B/ST5/01212 and the Bavarian State Ministry for Science and the Arts for the research program "Solar Technologies Go Hybrid"; funding from the European Research Council (ERC) under the European Union's Horizon 2020 research and innovation program (Grant agreements No. 949191 for E.G. and No. 787937 for F. W.); funding from the city council of Brno, Czech Republic; and the Knut and Alice Wallenberg Foundation.

Conflict of Interests

The authors declare no conflict of interest.

Data Availability Statement

The data that support the findings of this study are available in the supplementary material of this article.

Keywords: hydrogen peroxide · oxygen reduction reaction · perylene · photocatalysis · dyes/pigments

[1] K. Mase, M. Yoneda, Y. Yamada, S. Fukuzumi, *Nat. Commun.* **2016**, *7*, 11470.
[2] Y. Shiraishi, S. Kanazawa, Y. Kofuji, H. Sakamoto, S. Ichikawa, S. Tanaka, T. Hirai, *Angew. Chem. Int. Ed.* **2014**, *53*, 13454–13459.
[3] S. Fukuzumi, *Joule* **2017**, *1*, 689–738.
[4] E. Miglbauer, P. J. Wójcik, E. D. Głowacki, *Chem. Commun.* **2018**, *54*, 11873–11876.
[5] F. Lodola, V. Rosti, G. Tullii, A. Desii, L. Tapella, P. Catarsi, D. Lim, F. Moccia, M. R. Antognazza, *Sci. Adv.* **2019**, *5*, eaav4620.
[6] M. R. Antognazza, I. A. Aziz, F. Lodola, *Oxid. Met.* **2019**, *2019*, 2867516.
[7] F. Moccia, S. Negri, P. Faris, C. Ronchi, F. Lodola, *Vascul. Pharmacol.* **2022**, *144*, 106998.
[8] Y. Kofuji, Y. Isobe, Y. Shiraishi, H. Sakamoto, S. Tanaka, S. Ichikawa, T. Hirai, *J. Am. Chem. Soc.* **2016**, *138*, 10019–10025.
[9] R. E. Stephens, B. Ke, D. Trivich, *J. Phys. Chem.* **1955**, *59*, 966–969.
[10] P. Clechet, C. Martelet, J. R. Martin, R. Olier, *Electrochim. Acta* **1978**, *24*, 457–461.
[11] M. Jakešová, D. H. Apaydin, M. Sytnyk, K. Oppelt, W. Heiss, N. S. Sariciftci, E. D. Głowacki, *Adv. Funct. Mater.* **2016**, *26*, 5248–5254.
[12] M. Gryszel, M. Sytnyk, M. Jakešová, G. Romanazzi, R. Gabrielsson, W. Heiss, E. D. Głowacki, *ACS Appl. Mater. Interfaces* **2018**, *10*, 13253–13257.
[13] M. Gryszel, R. Rybakiewicz, E. D. Głowacki, *Adv. Sustainable Syst.* **2019**, *3*, 1900027.
[14] A. Nowak-Król, K. Shoyama, M. Stolte, F. Würthner, *Chem. Commun.* **2018**, *54*, 13763–13772.
[15] R. Renner, M. Stolte, J. Heitmüller, T. Brixner, C. Lambert, F. Würthner, *Mater. Horiz.* **2022**, *9*, 350–359.
[16] F. Würthner, C. R. Saha-Möller, B. Fimmel, S. Ogi, P. Leowanawat, D. Schmidt, *Chem. Rev.* **2016**, *116*, 962–1052.
[17] Z. Chen, M. G. Debije, T. Debaerdemaeker, P. Osswald, F. Würthner, *ChemPhysChem* **2004**, *5*, 137–140.
[18] Z. Chen, U. Baumeister, C. Tschierske, F. Würthner, *Chem. Eur. J.* **2007**, *13*, 450–465.
[19] E. Tenori, A. Colusso, Z. Syrgiannis, A. Bonasera, S. Osella, A. Ostric, R. Lazzaroni, M. Meneghetti, M. Prato, *ACS Appl. Mater. Interfaces* **2015**, *7*, 28042–28048.
[20] J. Seibt, V. Dehm, F. Würthner, V. Engel, *J. Chem. Phys.* **2007**, *126*, 164308.
[21] D. Görl, X. Zhang, F. Würthner, *Angew. Chem. Int. Ed.* **2012**, *51*, 6328–6348.
[22] J. S. Zigler, J. L. Lepe-Zuniga, B. Vistica, I. Gery, *Angew. Chem. Int. Ed.* **1967**, *21*, 282–287.
[23] W. Xing, M. Yin, Q. Lv, Y. Hu, C. Liu, J. Zhang, in *Rotating Electrode Methods and Oxygen Reduction Electrocatalysts* (Eds.: W. Xing, G. Yin, J. Zhang), Elsevier, Amsterdam, **2014**, pp. 1-31.
[24] O. Scialdone, A. Galia, C. Gattuso, S. Sabatino, B. Schiavo, *Electrochim. Acta* **2015**, *182*, 775–780.
[25] J. F. Pérez, A. Galia, M. A. Rodrigo, J. Llanos, S. Sabatino, C. Sáez, B. Schiavo, O. Scialdone, *Electrochim. Acta* **2017**, *248*, 169–177.
[26] I. Ghosh, T. Ghosh, J. I. Bardagi, B. König, *Science* **2014**, *346*, 725–728.
[27] Y. Xu, J. Zheng, J. O. Lindner, X. Wen, N. Jiang, Z. Hu, L. Liu, F. Huang, F. Würthner, Z. Xie, *Angew. Chem. Int. Ed.* **2020**, *59*, 10363–10367.
[28] Z. D. Draganić, I. G. Draganić, M. M. Kosanić, *J. Phys. Chem.* **1966**, *70*, 1418–1425.
[29] G. G. Kramarenko, S. G. Hummel, S. M. Martin, G. R. Buettner, *Photochem. Photobiol.* **2006**, *82*, 1634.
[30] C. Flors, M. J. Fryer, J. Waring, B. Reeder, U. Bechtold, P. M. Mullineaux, S. Nonell, M. T. Wilson, N. R. Baker, *J. Exp. Bot.* **2006**, *57*, 1725–1734.
[31] F. Yukruk, A. L. Dogan, H. Canpinar, D. Guc, E. U. Akkaya, *Org. Lett.* **2005**, *7*, 2885–2887.
[32] A. Blacha-Grzechnik, A. Drewniak, K. Z. Walczak, M. Szindler, P. Ledwon, *J. Photochem. Photobiol. A* **2020**, *388*, 112161.
[33] P. Carloni, E. Damiani, L. Greci, P. Stipa, F. Tanfani, E. Tartaglini, M. Wozniak, *Res. Chem. Intermed.* **1993**, *19*, 395–405.
[34] T. Ohyashiki, M. Nunomura, T. Katoh, *Biochim. Biophys. Acta Biomembr.* **1999**, *1421*, 131–139.
[35] H. Sies, *Redox Biol.* **2017**, *11*, 613–619.
[36] O. S. Abdullaeva, I. Sahalianov, M. S. Ejneby, M. Jakešová, I. Zozoulenko, S. I. Liin, E. D. Głowacki, *Adv. Sci.* **2022**, *9*, 2103132.
[37] C. M. Cardona, W. Li, A. E. Kaifer, D. Stockdale, G. C. Bazan, *Adv. Mater.* **2011**, *23*, 2367–2371.
[38] R. S. Kularatne, H. Kim, M. Ammanamanchi, H. N. Hayenga, T. H. Ware, *Chem. Mater.* **2016**, *28*, 8489–8492.
[39] J. Li, C. Yang, Y. Chen, W. Y. Lai, *New J. Chem.* **2016**, *40*, 8886–8891.
[40] T. Deligeorgiev, D. Zaneva, I. Petkov, I. Timcheva, R. Sabnis, *Dyes Pigm.* **1994**, *24*, 75–81.
[41] Z. Chen, A. Lohr, C. R. Saha-Möller, F. Würthner, *Chem. Soc. Rev.* **2009**, *38*, 564–584.

Manuscript received: April 4, 2023
Revised manuscript received: May 25, 2023
Accepted manuscript online: May 26, 2023
Version of record online: May 26, 2023

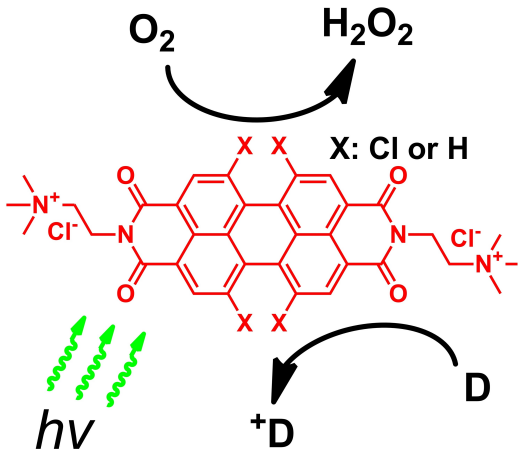

Dr. M. Gryszel, T. Schlossarek, Prof. F. Würthner, Prof. M. Natali, Dr. E. D. Głowacki**

Water-soluble dyes based on perylene diimide molecules were employed as molecular catalysts for the light-induced conversion of dissolved oxygen to hydrogen peroxide. Improved photocatalytic efficiency was achieved by using quaternary ammonium solubilizing units on the perylene diimide core and with selection of sacrificial electron donors.